

الجمهورية الجزائرية الديمقراطية الشعبية

République Algérienne Démocratique et Populaire

وزارة التعليم العالي والبحث العلمي

Ministère de l'Enseignement Supérieur et de la Recherche Scientifique

جامعة مولاي الطاهر، سعيدة

Université MOULAY Tahar, Saida



كلية العلوم

Faculté des Sciences

قسم الكيمياء

Département de Chimie

Mémoire pour l'obtention du diplôme de Master

En Chimie

Spécialité : Chimie Théorique et computationnelle

Thème

N° d'Ordre

**Understanding intermolecular interaction of the acceptor-donor  
complexe Trinitrobenzene(TNB)-Benzene.**

Présenté par :

■ M<sup>lle</sup> : BERRIAH Fatima Zohra

Soutenu le : 21/07/2023

Devant le jury composé de :

Président

Mr. RAHMOUNI Ali

Pr Univ MT Saida

Examinatrice

Mr. REINHOLD F. Fink

Pr Univ EK Tubingen, Germany

Rapporteur

M<sup>me</sup> SEKKAL Majda

Pr Univ DL Sidi Bel-Abbes

Année universitaire 2022/2023

# Contents

<b>1</b>	<b>Theoretical concepts</b>	<b>1</b>
1.1	Introduction	2
1.2	Intermolecular interactions terms	3
1.2.1	Electrostatic	3
1.2.2	induction	3
1.2.3	Dispersion	4
1.2.4	Exchange-repulsion	4
1.2.5	Charge transfert	4
1.3	Intermolecular interactions energy evaluation	4
1.3.1	Perturbation approach	5
1.3.2	Generalized perturbation method (SAPT)	5
<b>2</b>	<b>Results and Discussion</b>	<b>7</b>
2.1	Geometry optimisation	8
2.1.1	Geometry of monomers	8
2.1.2	Geometry of dimer	9
2.2	Decomposition of the intermolecular interaction energy for different shifts	10
2.2.1	Z-shift	10
2.2.2	X-shift	11
2.2.3	Y-shift	12
2.3	Rotation of trinitrobenzene around z-axis	13
2.4	Calculation of orbital contributions to the exchange-repulsion energy	15
2.4.1	Contribution of all orbitals to the exchange-repulsion energy	15
2.4.2	Contribution of $\pi - \pi$ orbitals to the exchange-repulsion energy	18
2.5	Potential surface of intermolecular interactions	19
2.6	conclusion	23

# List of Figures

2.1	Initial geometrical arrangement of TNB and Benzene from VESTA package.	9
2.2	Energy decomposition for the sandwich configuration of TNB-Benzene at the SAPT0/jun-cc-pVDZ level of theory with respect to the Z-shift from $z= 2\text{\AA}$ to $z= 6\text{\AA}$ .	10
2.3	Energy decomposition for the sandwich configuration of TNB-Benzene at the SAPT0/jun-cc-pVDZ along the x-axis from $x= 0\text{\AA}$ to $x= 6\text{\AA}$ .	11
2.4	Energy decomposition for the sandwich configuration of TNB-Benzene at the at the SAPT0/jun-cc-pVDZ level of the theory along the y-axis from $y= -6\text{\AA}$ to $y= 6\text{\AA}$ .	12
2.5	The arrangement of TNB-benzene stacks at $30^\circ$ from the VESTA package.	13
2.6	Variation of interaction energy, electrostatic, induction, dispersion and exchange-repulsion for the sandwich configuration of TNB-Benzene at the SAPT0/jun-cc-pVDZ level of theory with respect to the rotation around the $C_3$ axis.	14
2.7	Representation of $E_{exr}$ ( $\text{kJ.mol}^{-1}$ ) versus distance ( $\text{\AA}$ ) along the z-axis.	16
2.8	Representation of $E_{exr}$ ( $\text{kJ.mol}^{-1}$ ) versus distance ( $\text{\AA}$ ). Left: It is shifted along the x-axis. Right: It is shifted along the y-axis.	16
2.9	The three $\pi$ orbitals of benzene with the symmetry, each of them from the left, $e_{1gx}$ , $e_{1gy}$ and $a_{2u}$ .	17
2.10	Nine orbitals molecular $\pi$ of TNB with with symmetry, each of them from the top left $3e_y''$ , $3e_x''$ , $a_1''$ , $2e_x''$ , $2e_y''$ , $2a_2''$ , $1e_y''$ , $1e_x''$ and $1a_2''$ .	17
2.11	All orbitals $\pi - \pi$ Contribution of TNB-benzene to the exchange repulsion energy, left :along the x-axis. right:along the y-axis.	18
2.12	(Left: Contribution of orbital $e_{1gy}$ of benzene with $3e_x''$ (HOMO) of TNB. Right:Contribution of orbital $e_{1gy}$ (HOMO) of benzene with $2a_2''$ (HOMO-5)of TNB along the x-axis.	18
2.13	Contribution of orbital $e_{1gy}$ of benzene with $3e_y''$ (HOMO-1) of TNB.	19
2.14	Potential energy surface for the sandwich configuration at the SAPT0/jun-cc-pVDZ level of theory from the top left interaction, induction, electrostatic, dispersion, exchange-repulsion energies ( $\text{kJ.mol}^{-1}$ ) with respect to shift of the benzene molecule in the xy plane.	20
2.15	Contour plot of energy surface for the sandwich configuration at the SAPT0/jun-cc-pVDZ level of theory from the top left interaction, induction, electrostatic, dispersion, exchange-repulsion energies with respect to to shift of the benzene molecule in the xy plane.	21

## Acknowledgement

I would like to extend my sincere gratitude to all those who have supported and guided me throughout the journey of completing this master's thesis. This endeavor would not have been possible without the invaluable assistance and encouragement I received from various individuals .

To my parents, your constant belief in me and your sacrifices have been the driving force behind my academic pursuits. Your unwavering support has been my anchor, and I am forever grateful for your love and encouragement.

To my sisters, Nouara, Hanaa and Manel, your patience have been a source of motivation. I am sorry for all the trouble I was making. Thank you for your love and understanding.

I extend my deepest appreciation to my thesis advisors, Prof. Dr. Reinhold Fink from the Institute of Physical and Theoretical Chemistry at the University of Tübingen. Your mentorship, expertise, and dedication to my academic growth have been invaluable. Your guidance and feedback have significantly improved the quality of my research.

I also wish to express my gratitude to Prof. Dr. Rahmouni Ali from the Department of Chemistry at the University of Saïda. Your trust and encouragement were instrumental in my decision to participate in the Erasmus program.

A special thanks to the Ph.D. students Mr. Michael Thelen, Mr. Johannes Henrichsmeyer, and Dr. Stefan Behnle. Your collaboration and willingness to offer assistance have been instrumental in refining my research, despite your busy schedules.

To my friends in the lab, Fatima, Amel, Djamil and Julian, your support and shared experiences have made this academic journey both productive and enjoyable. Your friendship has lightened the load and brought joy to every challenge we have faced. I would also like to thank my friends in Algeria, Chaimaa and Hadil.

To all those who have played a role in my thesis journey, whether through encouragement, discussions, or simply being there when needed, thank you for contributing to this significant achievement.

## Abstract

Intermolecular interactions play a crucial role in numerous chemical and biological processes. Understanding the nature and strength of these interactions is essential for designing efficient materials and optimizing molecular interactions. In this work, the intermolecular interaction between trinitrobenzene and benzene are investigated at the SAPT0/jun-cc-pVDZ level of theory. Hereby, the interplanar distance is set to 3.5 Å which is optimal for or on top (sandwich) arrangement. Whole this structure turns out to be saddle point minima are found for structures where the benzene is shifted by about 1.1 Å within its molecular plane. Of particular interest in this investigation was the exchange-repulsion energy resulting from the overlapping occupied orbitals between the two monomers .

# **Chapter 1**

## **Theoretical concepts**

## 1.1 Introduction

The aggregation structure of condensed molecule systems is significantly influenced by intermolecular interactions. They are required for understanding chemical and physical properties of these substances. One of the most significant but least understood non-covalent interactions is that between aromatic groups. In this thesis ,the interaction of trinitrobenzene with benzene is investigated [8].

To gain a fundamental understanding of the many molecular interactions,many quanlita-tive and quantitative analytical methods have been proposed during the past few decades. Energy Decomposition Analysis (EDA) was first introduced by Morukuma and Kutura on the basis of Hartree Fock theory in 1970 [12].

In the present study, Symmetry Adapted Perturbation Theory (SAPT) is used as a theo-retical tool for estimating intermolecular interaction energies in terms of four physically significant components to the interaction energy: electrostatic, exchange-repulsion, in-duction and dispersion ,the analysis of the dimer was done at the SAPT0/jun-cc-pDVZ level of theory [6][16].

A main issue is the origin of molecular interaction as well as the problematic arrange-ment between these two monomers and this work, investigates the hypothesis that the exchange-repulsion is the controller of the intermolecular interaction [11].

As first part of the investigation into this hypothesis, trinitrobenzene-benzene will be stud-ied by changing the distance between the two monomers in the three directions of x,y and z.

The second part considers if that the exchange repulsion is the source of intermolecu-lar ineractions between molecules by studying the orbitals contribution to the exchange repulsion energy.

## 1.2 Intermolecular interactions terms

The interaction between two chemical entities is essentially due to the coulombic force, and it is under this aspect that it is generally studied. This does not exclude the existence of other forces, such as the gravity force, the strong nuclear and the weak nuclear force as well as other electromagnetic forces, but the latter have a very weak effect on molecules compared to the coulombic force.

The intermolecular interaction energy is composed of several terms, which were originally proposed to explain physicochemical phenomena.

### 1.2.1 Electrostatic

An electrostatic term can be attractive or repulsive and is the result of the interaction between permanent electric moments (charges, dipoles, quadruples, ...). If the distance between the interacting molecules is sufficiently large in relation to their dimensions, the electrostatic term can be expressed as the sum of the terms charges-charges, charge-dipoles, dipoles-dipoles, ..., written respectively in  $R^{-1}$ ,  $R^{-2}$ ,  $R^{-3}$ . In general, this term represents the main potential for interaction between two charged or polar chemical entities.

### 1.2.2 induction

The idea of polarisability. It is possible to express the total energy as a power series in the applied field by studying how the total energy,  $E$ , of a molecular system changes when an external homogeneous field,  $f$ , is applied. This gives the following expression:

$$E(f) = E_0 - \mu_0 f - f \alpha_0 f + \text{higher order terms} \quad (1.1)$$

The unperturbed energy is the first term on the right-hand side, followed by the interaction between the applied field and the dipole moment  $\mu_0$ , and finally the interaction between the applied field and the rearrangement in the charge distribution. The polarizability tensor,  $\alpha_0$ , which characterizes this term is quadratic in the applied field. It is referred to as the induction energy. The characteristics should be tested at the zero field, according to the subscript 0. We may write, "For an isotropic system,"[5]

$$E_{ind} = -\frac{1}{2} \alpha f^2 \quad (1.2)$$

In the presence of the field, the molecule dipole moment can be expressed as,

$$\mu = \mu_0 + \alpha_0 f \quad (1.3)$$

As a result, it is clear that polarizability links variations in molecule dipole moment to applied field. Similar terminology that links changes in the molecular quadrupole moment to the applied field gradient and other factors naturally exist. It is typically sufficient to take into account the first term in this expansion for tiny molecules.

### 1.2.3 Dispersion

Dispersion is an effect that is not easily understood in classical terms. It arises because the motions of the electrons in two molecules become correlated, favouring lower energy configurations and disfavouring higher energy ones. The dispersion energy depends on the ionisation potentials and polarisabilities of the interacting molecules and increases with molecular size and shape [2]. The interaction is called the dispersion interaction (also known as the London dispersion interaction, after London, who was the first to explain the phenomena). London derived the following expression for this interaction,

$$E_{disp}(a, b) = -\frac{3}{2} \frac{1}{r_{ab}^6} \alpha_a \alpha_b \frac{I_a I_b}{I_a + I_b} \quad (1.4)$$

$I_a$  is the ionisation potential of molecule a and  $\alpha_a$  the polarisability. To compare it with the dipole-induced dipole interaction, it depends the distance as  $r^{-6}$  [5].

### 1.2.4 Exchange-repulsion

The exchange-repulsion energy [49] is a non-additive and repulsive term that consists of two components. The exchange energy is a consequence of the fact that electron motions can extend over both molecules, and is an attractive term. The second term arises when the electrons attempt to occupy the same region of space, and are forced to redistribute because the Pauli exclusion principle forbids electrons of the same spin to be in the same space. Since the repulsion energy is approximately twice as large as the exchange energy, their sum is repulsive and it is actually the dominant contribution at short-range [19].

### 1.2.5 Charge transfert

Charge transfer is the donation of charge from one molecule to another. It is similar to covalent interactions in bonds, but between molecules and weaker. It decays exponentially with distance because it depends on orbital overlap, so it is expected to be important only in the short range. In the range where charge transfer is important, it can be difficult to distinguish from polarisation, as both are conceptually similar when the assignment of electrons to molecules is not clear [18].

On the other hand, charge transfer is an effect that can be also considered as part of the induction forces that act as short-range [15][2]. The charge transfer model was introduced by Mulliken in complexes that have an electron-rich (donor) and an electron-poor (acceptor) component [9][15]. The acceptor component strongly attracts electrons and therefore these complexes are also known as electron donor-acceptor complexes.

## 1.3 Intermolecular interactions energy evaluation

There are two different ways of calculating an intermolecular interaction energy. One is the supermolecular method, In the supermolecular method, the intermolecular interaction energy is the difference between the total energy of the dimer and the sum of the energies of each monomer:

$$\Delta E = E_{AB} - E_A - E_B \quad (1.5)$$

A and B denote the two monomers, and AB the dimer. The other method is the construction of an interaction by contributions directly from the wave functions of the separate monomers. In this thesis we use the second method because the direct calculation of an interaction energy by the supermolecular method gives no information about the nature of the interaction [3].

### 1.3.1 Perturbation approach

In this approach,[17] the total Hamiltonian  $H$  of the system is divided into the Hamiltonian  $H_0$  being the sum of the Hamiltonians of the isolated molecules,  $H_0 = H_A + H_B$ , and the intermolecular perturbation operator  $V = H - H_0$ . The interaction energy of two closed-shell molecules (A and B) is represented as

$$E_{int} = E_{pol}^{(1)} + E_{exch}^{(1)} + E_{ind}^{(2)} + E_{disp}^{(2)} + E_{exch}^{(2)} + E_{disp}^{(3)} + \dots \quad (1.6)$$

where  $E_{pol}^{(1)}$  is the classical electrostatic energy of the interaction of charge distributions of the unperturbed monomers;  $E_{ind}^{(2)}$  and  $E_{disp}^{(2)}$  are the induction and dispersion energies, respectively;  $E_{exch}^{(1)}$  and  $E_{exch}^{(2)}$  are the exchange components of the first and of the second order, respectively; and, finally,  $E_{disp}^{(3)}$  is the third-order dispersion correction. The induction and dispersion corrections are defined with the account of the damping caused by the charge overlap (penetration) effects. The induction energy describes the deformation of the electron charge distribution of one monomer by the electric field of the other, i.e., interactions of the permanent multipoles with the induced ones. The dispersion terms account for intersystem electron correlation. The exchange terms can be interpreted as resulting from quantum tunneling of electrons between the two systems. In the second order, the exchange term can be separated into the exchange-induction and exchange-dispersion components. Choosing the zeroth-order Hamiltonian to be the sum of the electrostatic Hamiltonians for the two separated atoms

$$H_0 = H_a(i) + H_b(j) \quad (1.7)$$

### 1.3.2 Generalized perturbation method (SAPT)

SAPT is a family of ab initio methods that directly compute the intermolecular interaction energy of a molecular dimer [11]. In all SAPT methods, the dimeric Hamiltonian,  $\hat{H}$  is defined as a sum of zeroth-order Hamiltonians for each monomer with an intermolecular interaction operator,

$$\hat{H} = \hat{H}_A + \hat{H}_B + \hat{V} \quad (1.8)$$

where A and B refer to each monomer and  $\hat{V}$  describes interactions between electrons and nuclei of one monomer with those of the other monomer.

The following SAPT [7] variations with increasing computational complexity are descended from the polarization expansion: SAPT0, SAPT2, SAPT2+, etc. The simplest approach, known as SAPT0, treats everything at the Hartree Fock (HF) level without taking intramolecular correlation into account.

$$E^{SAPT0} = E^{HF} + [E_{disp}^{(20)} + E_{exch-disp}^{(20)}]_{disp} \quad (1.9)$$

$$E^{SAPT2} = E^{SAPT0} + [E_{elst,r}^{(20)}]_{elst} + [E_{exch}^{(11)} + E_{exch}^{[12]}]_{exch} + [E_{ind}^{(22)} + E_{exch-ind}^{(22)}]_{ind} \quad (1.10)$$

$$E^{SAPT2+} = E^{SAPT2} + [E_{disp}^{(21)} + E_{disp}^{(22)}]_{disp} \quad (1.11)$$

$$E^{SAPT2+(3)} = E^{SAPT2+} + E_{elst,resp}^{(13)} + E_{30}^{(30)} \quad (1.12)$$

$$\delta E_{MP2} = E^{MP2} - E^{(SAPT2)} \quad (1.13)$$

$E^{(\mu\nu)}$  with  $\mu, \nu = 0, 1, 2, \dots$  represents the expansion term with superscripts indicating the intermolecular order ( $\mu$ ) and summed intramolecular order ( $\nu$ ) from either monomer A or monomer B.  $E^{MP2}$  is the interaction energy at the MP2 level using supermolecular approach, which is CP corrected. Currently, implementation of SAPT usually starts with the wave function as product of two monomers, because the wave function should be antisymmetric, corrections due to exchange effect are included in above equations with subscripts *exch*.

The simplest SAPT method[11], SAPT0, is defined as being second-order in  $v$ , and zeroth-order in  $w$ ,

$$\begin{aligned} E_{int}^{SAPT0} = & [E_{elst}^{(10)}]_{elst} + [E_{exch}^{(10)}]_{exch} \\ & + [E_{ind,r}^{(20)} + E_{exch;ind,r}^{(20)} + \delta E_{HF}^{(2)}]_{ind} \\ & + [E_{disp}^{(20)} + E_{exch,disp}^{(20)}]_{disp} \end{aligned} \quad (1.14)$$

They use square brackets simply to organize terms into the four component types. In equation (1.14), we also introduce a  $\delta E_{HF}^{(2)}$  correction. For SAPT methods that are second-order in  $v$ , some higher-order effects (primarily induction-like) can be implicitly captured by including the Hartree–Fock (HF) interaction energy,  $E_{IE}^{(HF)}$ , computed according to Equation 1. Specifically, we define a second-order HF correction ( $\delta E_{HF}^{(2)}$ ) as the difference between the HF interaction energy and a dispersion-less SAPT interaction energy with  $v = 2$  and  $w = 0$ ,

$$\delta E_{HF}^{(2)} = E_{IE}^{(HF)} - ([E_{elst}^{(10)}]_{elst} + [E_{exch}^{(10)}]_{exch} + [[E_{ind,r}^{(20)} + E_{exch-ind,r}^{(20)}]_{ind}]). \quad (1.15)$$

## **Chapter 2**

# **Results and Discussion**

## 2.1 Geometry optimisation

### 2.1.1 Geometry of monomers

To investigate the case of intermolecular interaction between the two monomers (trinitrobenzene-benzene), we do the optimisation of each monomer with MP2 level of theory and aug-cc-pVTZ basis set using Turbomole package [1] and ORCA programme [10]. with respect to the symmetry of the monomers  $D_{3h}$  for trinitrobenzene and  $D_{6h}$  for benzene. The bond distances and optimised angles are listed in tables 2.1 and 2.2, these results are consistent with those obtained by comparing the experimental results of the single crystal structure of trinitrobenzene bond distances and angles.

Table 2.1: Lists the equilibrium intermonomer distances of trinitrobenzene in ( $\text{\AA}$ ) for single crystal structure of TNB [4] and the theoretical MP2/aug-cc-pVTZ data.

Distances ( $\text{\AA}$ )	experimental	theoretical
$C - C$	1.385	1.386
$C - N$	1.50	1.477
$N - O$	1.23	1.227

Table 2.2: Lists the equilibrium angles of trinitrobenzene in degree ( $^\circ$ ) in a single crystal structure [4] and the theoretical MP2/aug-cc-pVTZ.

Angles( $^\circ$ )	experimental	theoretical
$O - N - O$	127.1	126.0
$O - N - C$	117.8	116.9

## 2.1.2 Geometry of dimer

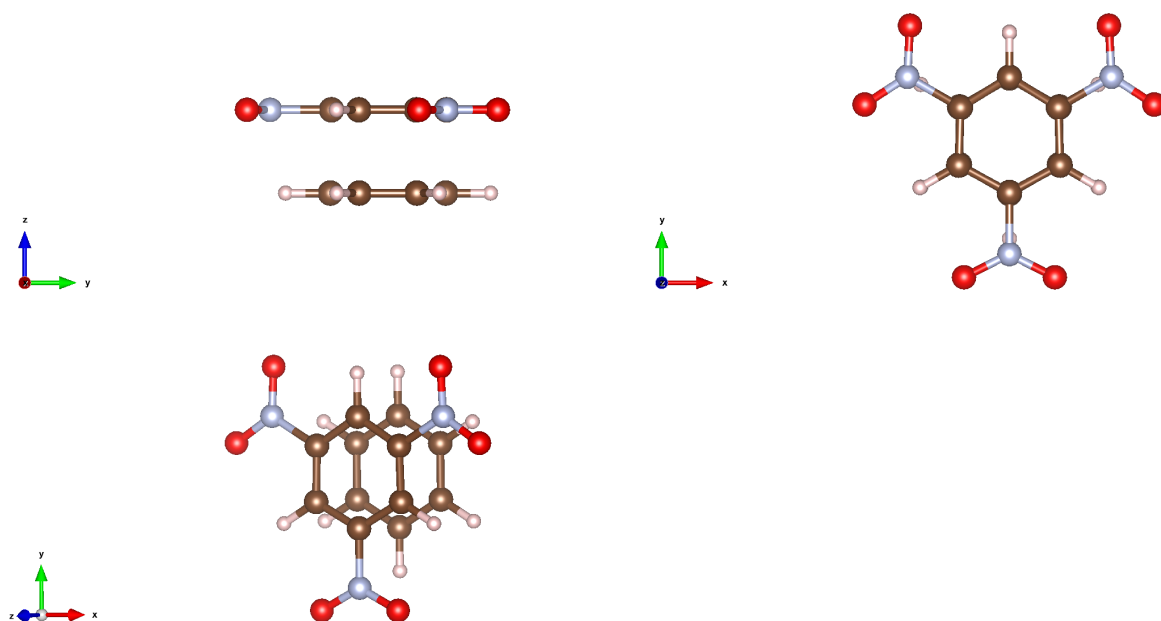


Figure 2.1: Initial geometrical arrangement of TNB and Benzene from VESTA package.

The calculation were conducted at the SAPT0 level of theory with the jun-cc-pVDZ basis using the PSI4 program [14], we put the two monomers in a sandwich configuration, so that the main axis is the  $C_3$  axis which runs along the Z-axis and the X-axis is placed between the group of nitro and the atom of hydrogen of the trinitrobenzene and for the Y-axis is placed up where the atom of hydrogen is between the two groups of nitro.

## 2.2 Decomposition of the intermolecular interaction energy for different shifts

### 2.2.1 Z-shift

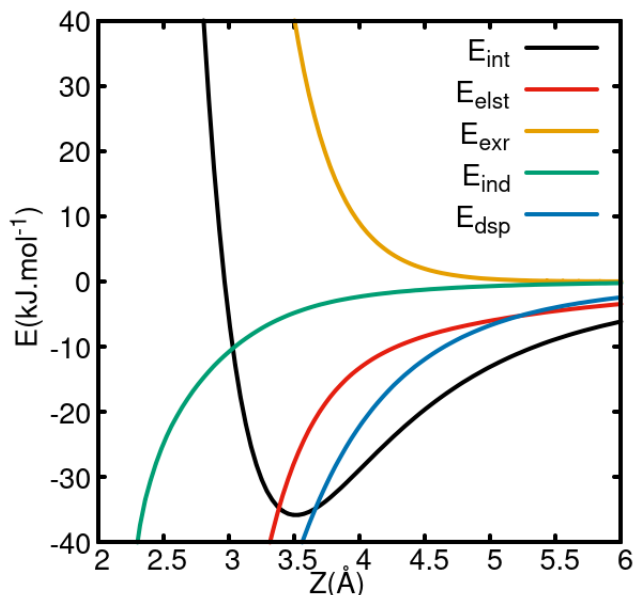


Figure 2.2: Energy decomposition for the sandwich configuration of TNB-Benzene at the SAPT0/jun-cc-pVDZ level of theory with respect to the Z-shift from  $z=2\text{\AA}$  to  $z=6\text{\AA}$ .

Energies	$E_{int}$	$E_{elst}$	$E_{exr}$	$E_{ind}$	$E_{disp}$
$z=3.5\text{\AA}$	-35.81	-27.84	40.50	-4.826	-43.65

Table 2.3: Lists the values of intermolecular energies ( $\text{kJ.mol}^{-1}$ ) at the minimum  $z=3.5\text{\AA}$ .

Figure (2.3) represents the variation of the total intermolecular energy along the z-axis, it seems that the interaction energy has a minimum around  $E=-35.81 \text{ kJ.mol}^{-1}$ . For this motion the two monomers prefer to stay at distance  $z=3.5 \text{ \AA}$ . As the changes in distance intermonomers from benzene dimer has  $3.7 \text{ \AA}$  [13] to the distance between trinitrobenzene-benzene dimer, this optimum intermonomer distance agrees with the notion that when benzene is more substituted this result in a decrease in the distance between the two monomers, this was indicated in a work in which a distance was compared between benzene molecules and other benzene substituted in stacking mode [11]. Given the curve of intermolecular interaction before the region of minimum the rapid decrease of energy with small variation of distance indicate that there is a force making the two monomers for enough away. Table (2.3) summarises the values of energies at the minimum and shows that the dispersion energy is the most attractive energy contribution. However, for  $z$  larger then  $5 \text{ \AA}$  the electrostatic energy becomes the most attractive one. For the induction energy, the increased energy is shown before the minimum of the intermolecular interaction where it gets less attractive at the minimum with value of energy

$E = -4.83 \text{ kJ.mol}^{-1}$ . The exchange-repulsion is rapidly decreasing with increasing  $z$  and at  $z = 4.7 \text{ \AA}$  the exchange-repulsion energy is essentially zero. It can be concluded that when TNB and benzene are in  $z$  coordinate distance longer than  $4.7 \text{ \AA}$  there is no significant exchange-repulsion interaction.

## 2.2.2 X-shift

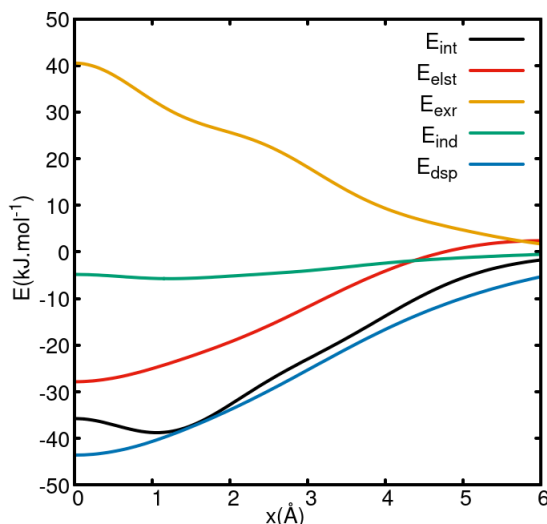


Figure 2.3: Energy decomposition for the sandwich configuration of TNB-Benzene at the SAPT0/jun-cc-pVDZ along the  $x$ -axis from  $x = 0 \text{ \AA}$  to  $x = 6 \text{ \AA}$ .

Table 2.4: Values of intermolecular energy and its contributions ( $\text{kJ.mol}^{-1}$ ) for  $x = 0 \text{ \AA}$  and at the minimum  $x = 1.1 \text{ \AA}$  of TNB-benzene and the energy differences between these structures.

Energies	$E_{int}$	$E_{elst}$	$E_{exr}$	$E_{ind}$	$E_{dsp}$
$x = 0 \text{ \AA}$	35.74	-27.84	40.51	-4.83	-43.58
$x = 1.1 \text{ \AA}$	-38.75	-24.52	31.57	-5.71	-40.08
$\Delta E$	-3.01	3.32	-8.94	-0.88	3.5

After the determination of the favourable distance between the two monomers  $z = 3.5 \text{ \AA}$ , we consider how the intermolecular interaction changes along the  $x$ -axis. This is represented in figure (2.3) which shows for the intermolecular energy a minimum at  $E = -38.75 \text{ kJ.mol}^{-1}$  for  $x = 1.1 \text{ \AA}$ .

Table (2.4) summarises of energies in the stacking mode ( $x = 0 \text{ \AA}$ ) and at the minimum ( $x = 1.1 \text{ \AA}$ ). The difference of the interaction energy is  $\Delta E = 3.01 \text{ kJ.mol}^{-1}$ .

The behaviour of electrostatic and dispersion energies is similar, the increasing smoothly with approximately the same difference of energy between stacking mode and the energy at  $x = 6 \text{ \AA}$ .

Induction energy changes only slightly and the difference energy proves  $\Delta E = 0.88 \text{ kJ.mol}^{-1}$ .

It is a bit difficult to determine the region where the exchange-repulsion varies significantly as it decays consistently with increasing  $x$ . However in the region  $x=1.1 \text{ \AA}$  there is a notable sholder in this interaction contribution.

### 2.2.3 Y-shift

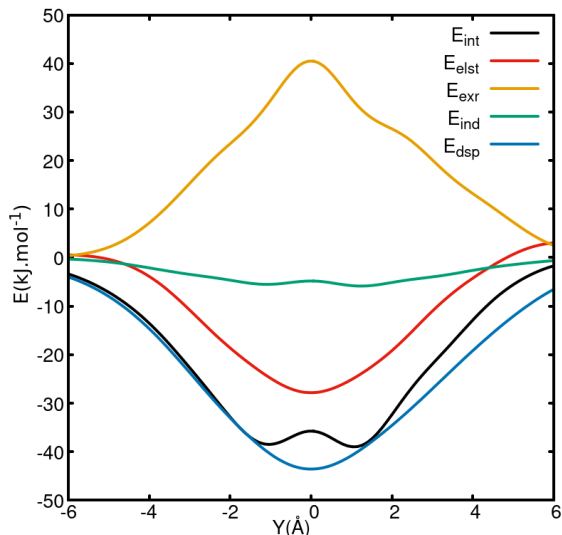


Figure 2.4: Energy decomposition for the sandwich configuration of TNB-Benzene at the SAPT0/jun-cc-pVDZ level of the theory along the y-axis from  $y= -6\text{\AA}$  to  $y= 6\text{\AA}$ .

Table 2.5: values of intermolecular energies ( $\text{kJ.mol}^{-1}$ ) along the y-axis at  $y=0\text{\AA}$  and at the minimum  $y=1.1\text{\AA}$  , $y= -1 \text{\AA}$  of TNB-benzene .

Energies	$E_{int}$	$E_{elst}$	$E_{exr}$	$E_{ind}$	$E_{disp}$
$y=0\text{\AA}$	-35.74	-27.84	40.51	-4.83	-43.58
$y=1.1\text{\AA}$	-38.99	-24.65	31.76	-5.85	-40.27
$y=-1\text{\AA}$	-38.49	24.87	32.38	-5.51	-40.49

The objective to describe the intermolecular interaction energy along y-axis from  $y=-6 \text{ \AA}$  to  $y=6 \text{ \AA}$  is the location of the group nitro in negative part of y-axis for give a closely look of variation energy between the two monomers.

At the first glance the curves in figure (2.4) appear symmetrical but the energies in table (2.5) show that the global minimum of intermolecular interaction is present around  $E=-38.99 \text{ kJ.mol}^{-1}$  at  $y=1.1 \text{ \AA}$  and continue at long range increasing smoothly the curves of electrostatic and dispersion energy where the two latter energies represent the small value of energies at  $y= -1 \text{ \AA}$  (negative region) with  $E_{elst}=-24.87 \text{ kJ.mol}^{-1}$  and  $E_{dsp}=-40.49 \text{ kJ.mol}^{-1}$ .

With the comparison of the small difference of value energies of induction ,it can be possible to say that the induction energy at  $y=1.1 \text{ \AA}$  has value  $E_{ind}= -5.85 \text{ kJ.mol}^{-1}$ .

The comparison of exchange-repulsion curve between the negative part and the positive part. shows that exchange-repulsion energy contains a variation at the minimum located in the positive part  $y=1.1 \text{ \AA}$  where the decreasing of this energy is rapid. It can be observed between  $y=0.4 \text{ \AA}$ - $1.7 \text{ \AA}$ .

### 2.3 Rotation of trinitrobenzene around z-axis

In this section we study the intermolecular interaction energy, but with the rotation of TNB around the Z ( $C_3$ ) axis for only  $60^\circ$ , due to the symmetry of trinitrobenzene, and without changing the distance between the two monomers ( $Z=3.5 \text{ \AA}$ ), which is found to be the most favoured separation between two rings of monomers.

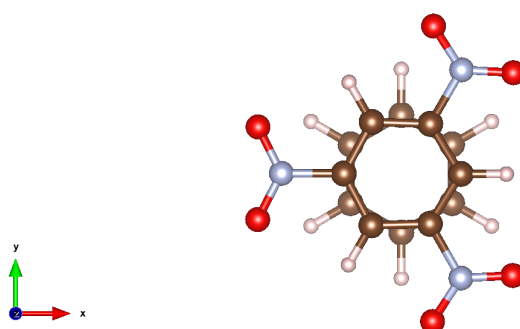


Figure 2.5: The arrangement of TNB-benzene stacks at  $30^\circ$  from the VESTA package.

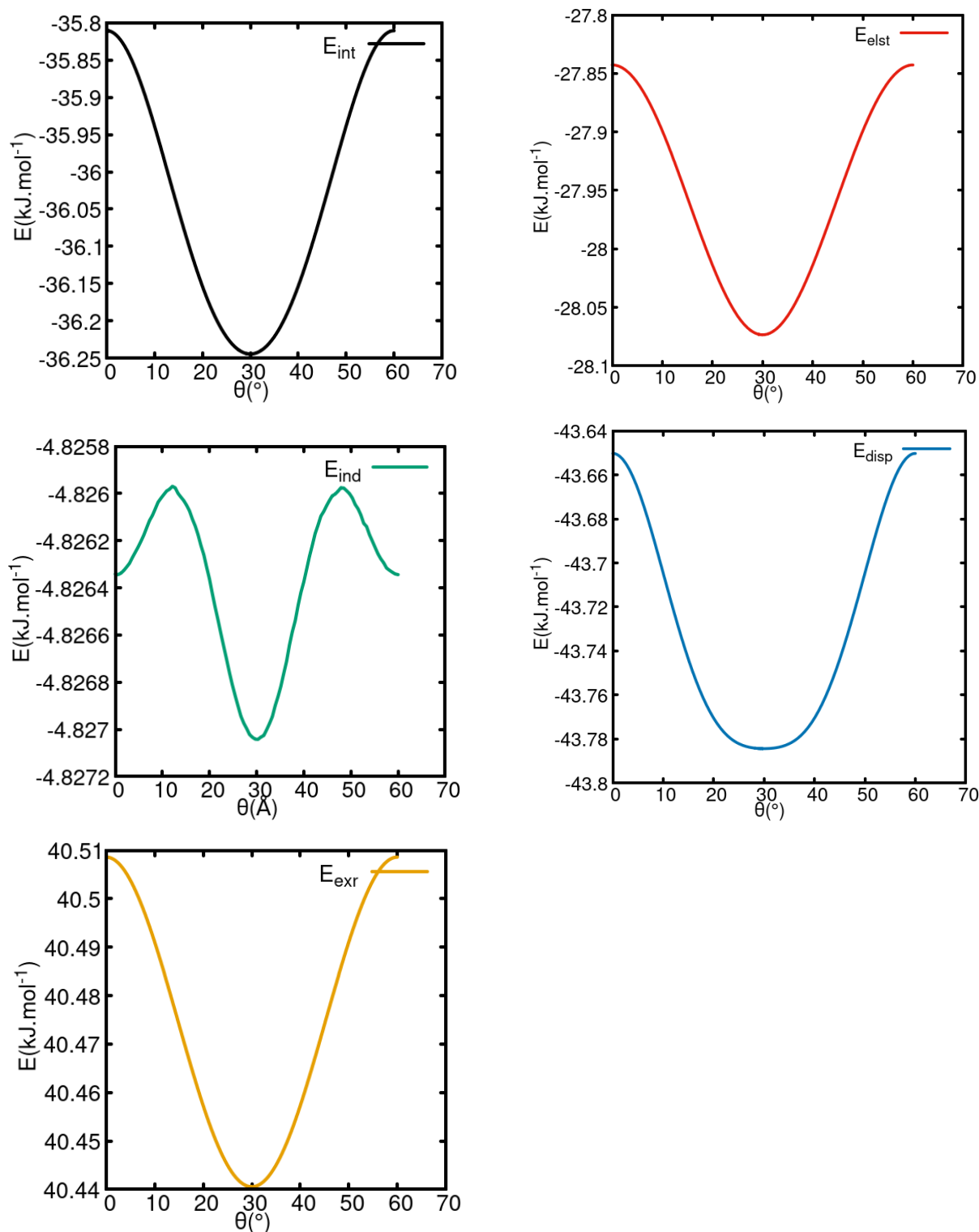


Figure 2.6: Variation of interaction energy, electrostatic, induction, dispersion and exchange-repulsion for the sandwich configuration of TNB-Benzene at the SAPT0/jun-cc-pVDZ level of theory with respect to the rotation around the  $C_3$  axis.

Figure 2.6 shows the variation of the intermolecular interaction energy with the rotation angle as well as the, electrostatic, induction, dispersion and exchange-repulsion respectively.

We see the minimum of the intermolecular interaction energy around  $E=-36.24 \text{ kJ.mol}^{-1}$  at  $30^\circ$ , where the atoms of the nitro group are located by projection in the middle of the benzene bond that is shown in the figure 2.5. This arrangement represents the most stable geometry between the two monomers with a difference of  $0.4 \text{ kJ.mol}^{-1}$ . If we compare the intermolecular interaction energy obtained for rotating the TNB-benzene as shown in table 2.6 below. We find that it does not change by more than  $0.5 \text{ kJ.mol}^{-1}$  which is essentially negligible.

Table 2.6: The table shows the difference energies ( $\text{kJ.mol}^{-1}$ ) between the stacking geometry and the rotational geometry around the  $C_3$  axis (Z) of TNB-benzene at ( $Z=3.5\text{\AA}$ ).

Energies	stacking geometry	rotation geometry	Difference energies
$E_{int}$	-35.81	-36.24	0.43
$E_{elst}$	-27.84	-28.07	0.23
$E_{exr}$	40.50	40.44	0.06
$E_{ind}$	-4.826	-4.827	0.001
$E_{disp}$	-43.65	-43.78	0.13

## 2.4 Calculation of orbital contributions to the exchange-repulsion energy

### 2.4.1 Contribution of all orbitals to the exchange-repulsion energy

The aim of choosing the interaction exchange-repulsion is to make it easier to understand how these monomers arrange between them, the calculation orbitals contributions explain the features of the exchange repulsion energy.

All calculations to obtain the exchange -repulsion energy between total orbitals of each monomer were carried out using the wavel program which employs SAPT0 method with jun-cc-pVDZ basis set .

In this calculation, the distance between the two monomers was shifted along the z-axis from  $z=2\text{\AA}$  to  $z=6\text{\AA}$  with 0.1 increment. Then it shifted by steps of  $0.1\text{\AA}$  along the x-axis and y-axis. The final position in both cases is  $6.0\text{\AA}$  with a constant  $z=3.5\text{\AA}$  .

For the negative part of the y-direction, they have not been taken into account for their existence of a global minimum in the positive part of the y-direction.

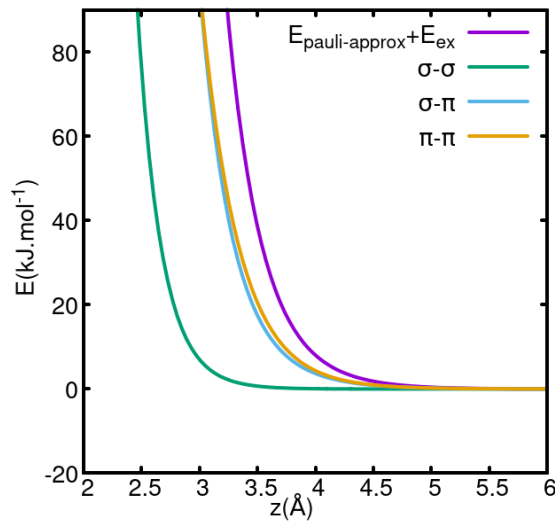


Figure 2.7: Representation of  $E_{exr}$  ( $kJ.mol^{-1}$ ) versus distance ( $\text{\AA}$ ) along the z-axis.

The variation of the exchange-repulsion along the z-axis is only the decrease of the energy with the increase of the distance between the two monomers and indicates that the  $\sigma - \sigma$  contributions to  $E_{exr}$  are much weaker than the roughly similar  $\sigma - \pi$  and  $\pi - \pi$  contributions.

It can be observed that at  $z=4.5\text{\AA}$ ,  $E_{exr}$  is approximately zero and it can be observed that the total  $\sigma - \sigma$  contribution so far  $z \leq 3.3\text{\AA}$ , It can be neglected if it is compared with the total  $\sigma - \pi$  and total  $\pi - \pi$  contributions at  $z=3.5\text{\AA}$ .

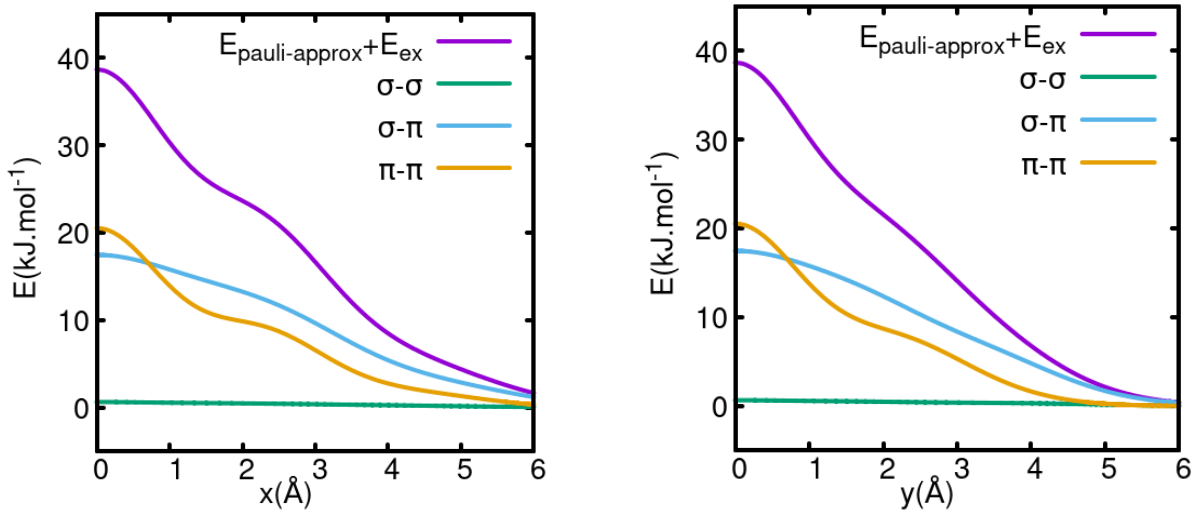


Figure 2.8: Representation of  $E_{exr}$  ( $kJ.mol^{-1}$ ) versus distance ( $\text{\AA}$ ). Left: It is shifted along the x-axis. Right: It is shifted along the y-axis.

The figure 2.8 shows the variation of the orbital contributions to the exchange-repulsion energy. As we can see the three different types of contribution:  $\sigma - \sigma$ ,  $\sigma - \pi$  and  $\pi - \pi$ . The first observation from the calculation of the total exchange-repulsion that the total  $\pi - \pi$  is the dominant contribution with energy  $E=20.51kJ.mol^{-1}$  at  $x=0\text{\AA}$ , this latter representing 50% of the total exchange-repulsion energy at  $x=0\text{\AA}$ . It shows such a pattern as

the total  $E_{\text{exr}}$ . The  $\sigma - \sigma$  contributions do not change along the variation of  $x$  or  $y$  and are negligible.

As mentioned above the most important orbital contributions are of  $\pi - \pi$  type. To study the contribution of the exchange-repulsion energy of each molecular  $\pi$  orbital of TNB with each molecular  $\pi$  orbital of benzene these are first shown in the figures 2.8 and 2.9.

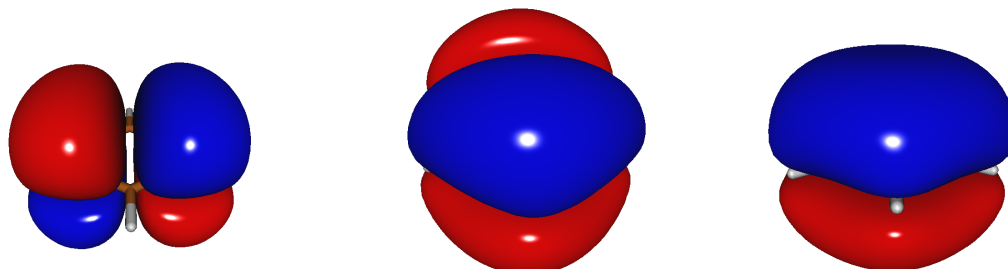


Figure 2.9: The three  $\pi$  orbitals of benzene with the symmetry, each of them from the left  $e_{1gx}$ ,  $e_{1gy}$  and  $a_{2u}$ .

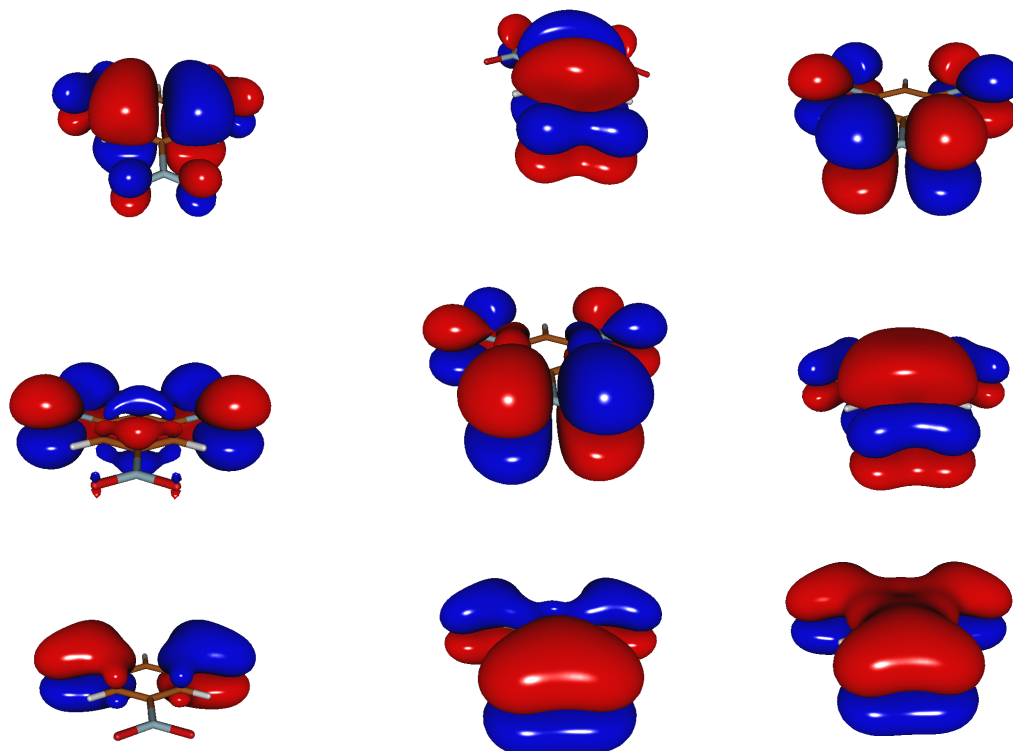


Figure 2.10: Nine orbitals molecular  $\pi$  of TNB with with symmetry, each of them from the top left  $3e''_y$ ,  $3e''_x$ ,  $a''_1$ ,  $2e''_x$ ,  $2e''_y$ ,  $2a''_2$ ,  $1e''_y$ ,  $1e''_x$  and  $1a''_2$ .

## 2.4.2 Contribution of $\pi - \pi$ orbitals to the exchange-repulsion energy

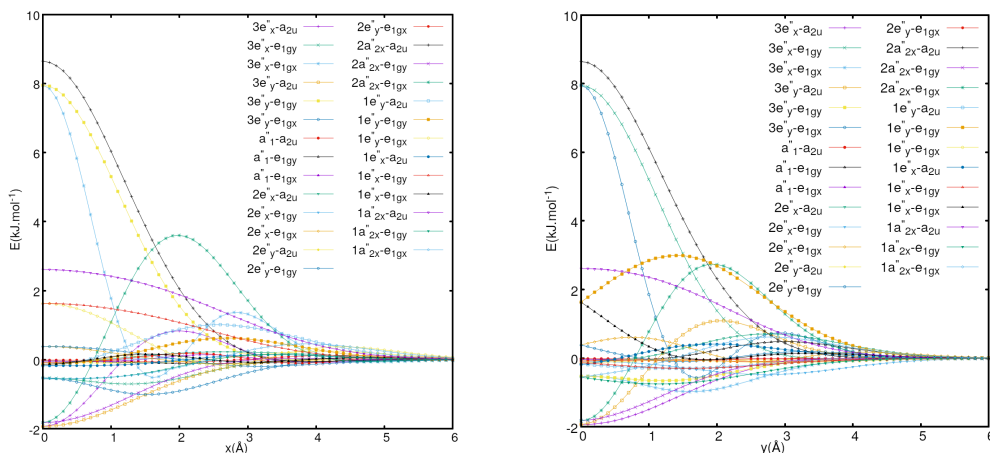


Figure 2.11: All orbitals  $\pi - \pi$  Contribution of TNB-benzene to the exchange repulsion energy, left :along the x-axis. right:along the y-axis.

It is possible to observe the energy contribution of the interaction between the nine  $\pi$  molecular orbitals of TNB and the three  $\pi$  molecular orbitals of benzene in the figure 2.11. To facilitate the study, it can be divided into three regions: a repulsive contribution, an attractive contribution and a zero contribution region where there is any variation. We will only study contributions that contain a change from repulsive to be attractive and vice versa because they are the main actors in the exchange -repulsion energy.

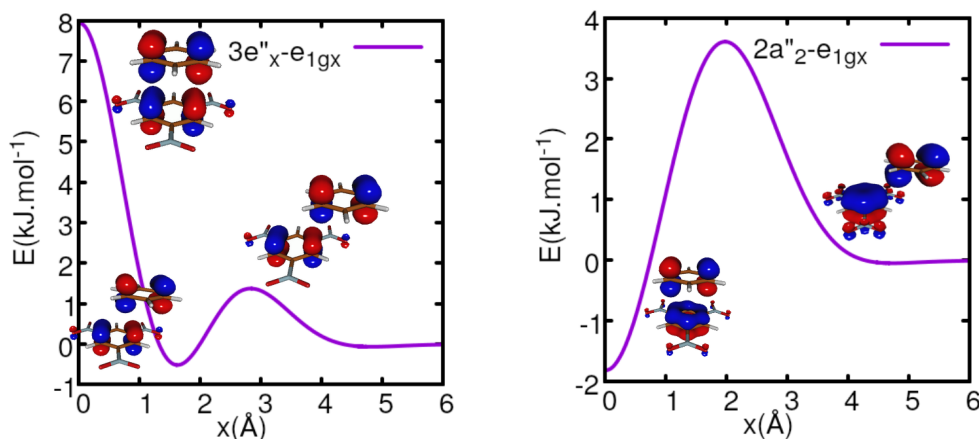


Figure 2.12: (Left: Contribution of orbital  $e_{1gy}$  of benzene with  $3e_x''$  (HOMO) of TNB. Right:Contribution of orbital  $e_{1gy}$  (HOMO) of benzene with  $2a_2''$  (HOMO-5)of TNB along the x-axis.

When benzene is shifted along the x-axis, most of the contribution to the  $E_{exr}$  is between the orbitals ( $3e_x''$  and  $2a_2''$ ) of TNB with the orbital ( $e_{1gx}$ ) of benzene. Due to the symmetry of the systems, which includes two mirror planes and the  $C_2$  axis as a symmetry element, the overlap of the orbital ( $3e_x''$ ) of TNB with the orbital ( $e_{1gx}$ ) of benzene at  $x=0 \text{ \AA}$  causes a maximum repulsive energy that means a greater overlap between the two orbitals.

Then at  $x=1.7 \text{ \AA}$  the orbital overlap becomes zero and the contribution to  $E_{exr}$  shows a minimum. However it increase with  $x$  leading to a maximum at  $x=2.8 \text{ \AA}$  with  $E= 1.5 \text{ kJ.mol}^{-1}$ .

For the contribution between the orbital ( $2a_2''$ ) of TNB and ( $e_{1gx}$ ) of benzene it starts with attractive energy due to zero overlap between the orbitals, because the orbital ( $2a_2''$ ) of TNB has node in the  $yz$  plane and the orbital ( $e_{1gx}$ ) has no node in the  $yz$  or  $xz$  planes this gives a zero overlap between them at  $x=0 \text{ \AA}$  and an overlap when the  $x$  increases leading to a repulsive maximum at  $x=2 \text{ \AA}$ . At  $x=4 \text{ \AA}$  the energy becomes negligible due to the separation of the two monomers.

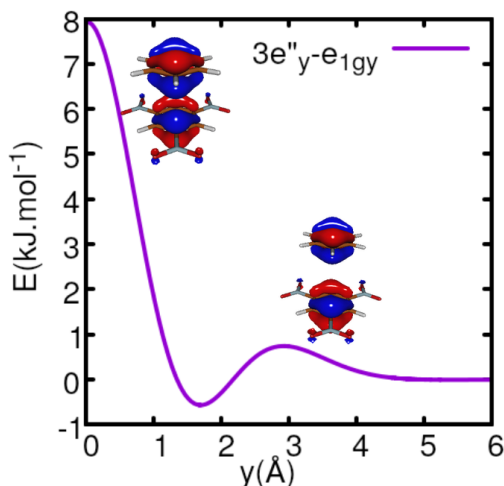


Figure 2.13: Contribution of orbital  $e_{1gy}$  of benzene with  $3e_y''$  (HOMO-1) of TNB.

Examining the contribution between the  $x$ -axis and the  $y$ -axis looks similar in terms of the format of the curves, but the only change is in the values of the energies, as shown in the figures 2.12 and 2.13.

The case of the contribution between the orbitals ( $3e_y''$ ) of TNB and ( $e_{1gy}$ ) of benzene along the  $y$ -axis contain the same explanation as the contribution of orbitals ( $3e_x'' - e_{1gy}$ ) along the  $x$ -axis, that it has a maximum repulsion due to strong overlapping at  $y=0 \text{ \AA}$  and decreases to an attractive minimum at  $y=1.7 \text{ \AA}$ .

## 2.5 Potential surface of intermolecular interactions

The aim of the potential surface is to describe the intermolecular interaction in the  $xy$  plane when the distance  $x$  and  $y$  varies between two monomers.

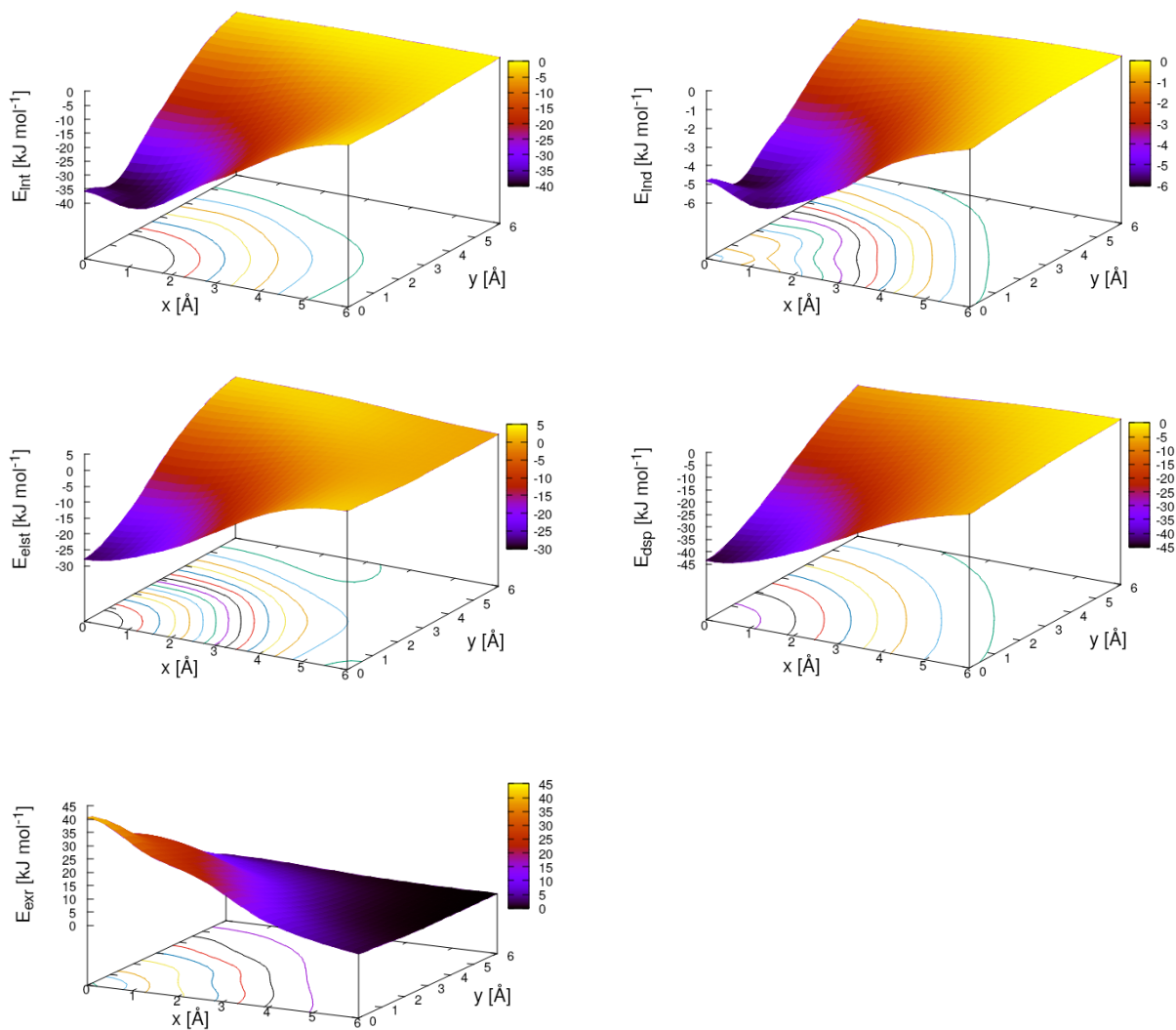


Figure 2.14: Potential energy surface for the sandwich configuration at the SAPT0/jun-cc-pVDZ level of theory from the top left interaction, induction, electrostatic, dispersion, exchange-repulsion energies ( $\text{kJ}\cdot\text{mol}^{-1}$ ) with respect to shift of the benzene molecule in the xy plane.

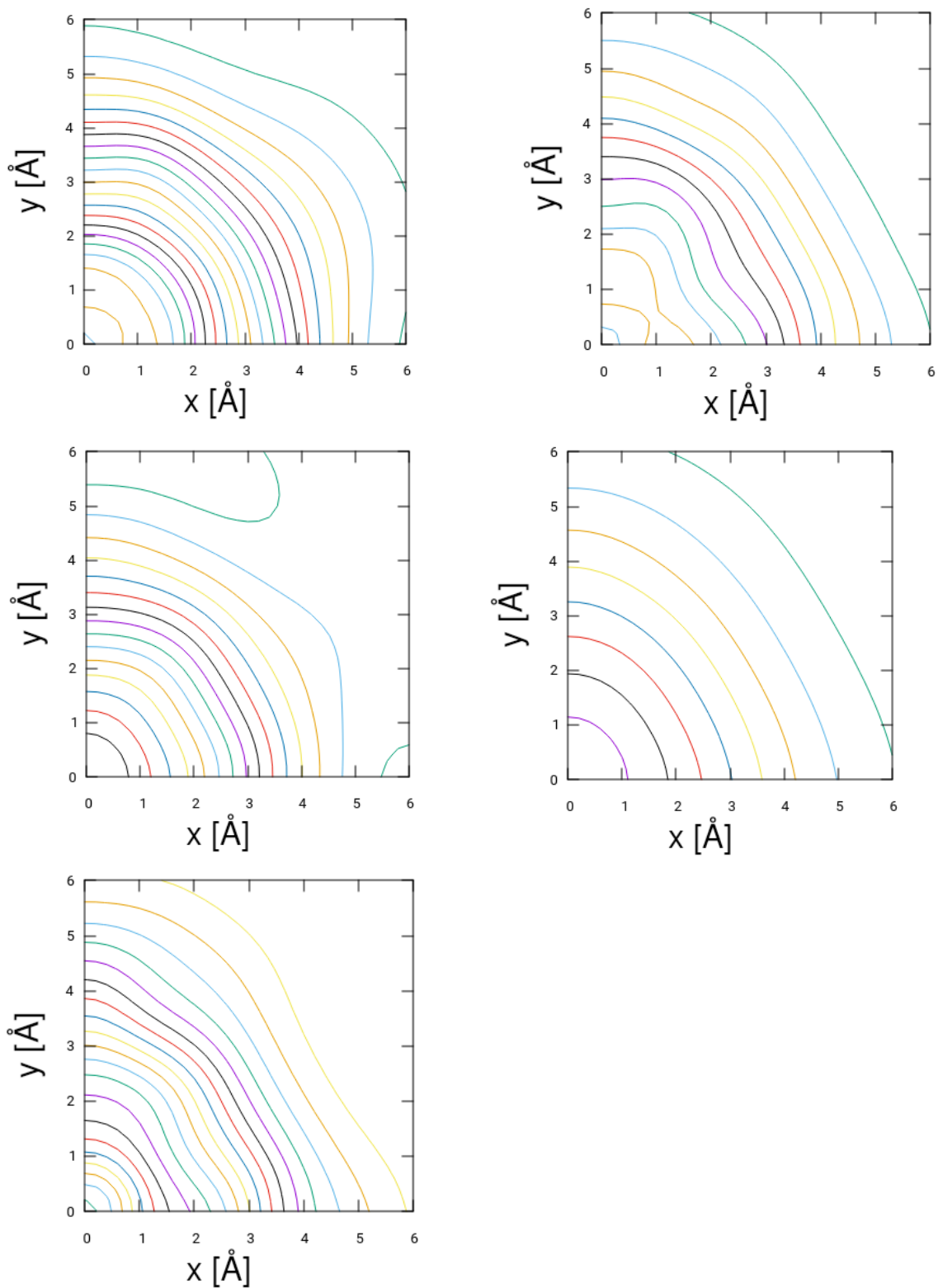


Figure 2.15: Contour plot of energy surface for the sandwich configuration at the SAPT0/jun-cc-pVDZ level of theory from the top left interaction, induction, electrostatic, dispersion, exchange-repulsion energies with respect to shift of the benzene molecule in the xy plane.

It is possible to see in figure (2.15) that there is no minimum in the xy plane but there is a minimum in x direction and another in y direction, these minima have very similar interaction energies which can be found in the table (2.7) below.

Table 2.7: The table shows the minimum of the potential surface of interaction energy ( $\text{kJ.mol}^{-1}$ ) with respect to the distances in ( $\text{\AA}$ ) of plane xy.

$x(\text{\AA})$	$y(\text{\AA})$	$E_{int}(\text{kJ.mol}^{-1})$
1.0	0.0	-38.74
0.0	1.0	-38.96

For the induction energy, despite small energy values, they contain a minimum at x direction and another at y direction, this variation of energy shown in table (2.8).

Table 2.8: The table shows the minimum of the potential surface of the induction energy ( $\text{kJ.mol}^{-1}$ ) with respect to the distances in ( $\text{\AA}$ ) of plane xy.

$x(\text{\AA})$	$y(\text{\AA})$	$E_{ind}(\text{kJ.mol}^{-1})$
1.2	0.0	-5.73
0.0	1.2	-5.86

With a minor energy difference between the two directions in the table (2.7), it is possible to state that the global minimum represents in the y direction; the same is true for induction, where a global minimum exists at  $y=1.2 \text{\AA}$  as shown in the table(2.8).

The variation of the exchange repulsion from a higher value of repulsion to a small value when moving away from  $x=y=0 \text{\AA}$  in the xy plane is more pronounced in the y direction than the x direction which can be seen, in figure(2.14).

The contour plot in the figure (2.15) of the dispersion energy represents an equal distributions of the energy between the x-direction and y-direction increasing rapidly of the energy, the same is found for the electrostatic energy ,but with a weaker increasing energy.

## 2.6 conclusion

In this thesis ,we explored how TNB and benzene arrange in planar displaced configurations for  $z=3.5 \text{ \AA}$  and we found that the TNB-benzene dimer interaction energy shows two minima with lowest one at  $E= -38.99 \text{ kJ.mol}^{-1}$  at  $y=1.1 \text{ \AA}, x=0 \text{ \AA}$  and a slightly higher one  $E= -38.75 \text{ kJ.mol}^{-1}$  at  $y=0 \text{ \AA} x=1.1 \text{ \AA}$ .

In view of the results presented in the section of calculation of exchange-repulsion, we concluded that the exchange-repulsion interaction allow to understand how the two molecules interact. We see that when the benzene shifted along the x-axis the orbitals that contribute most to the energy exchange-repulsion are:  $(3e''_x, e_{1gx})$  and  $(2a''_2, e_{1gx})$ .

When it is shifted along the y-axis,  $(3e''_y, e_{1gy})$  contributes the most.

# Bibliography

- [1] TURBOMOLE V7.2 2017, a development of University of Karlsruhe and Forschungszentrum Karlsruhe GmbH, 1989-2007, TURBOMOLE GmbH, since 2007; available from <http://www.turbomole.com>.
- [2] Alba Campo Cacharrón. *On the interaction between ions and complex aromatic systems*. PhD thesis, Universidade de Santiago de Compostela, 2014.
- [3] Edrisse Chermak. *Orbitales localisées pour les interactions intermoléculaires*. PhD thesis, Université Pierre et Marie Curie - Paris VI, 2, 2012.
- [4] Chang Sun Choi and James E Abel. The crystal structure of 1, 3, 5-trinitrobenzene by neutron diffraction. *Acta Crystallographica Section B: Structural Crystallography and Crystal Chemistry*, 28(1):193–201, 1972.
- [5] B. Jönsson G. Karlström. Intermolecular interactions. February 6, 2013.
- [6] Christian P Hettich, Xiaoyong Zhang, David Kemper, Ruoqi Zhao, Shaoyuan Zhou, Yangyi Lu, Jiali Gao, Jun Zhang, and Meiyi Liu. Multistate energy decomposition analysis of molecular excited states. *JACS Au*, 2023.
- [7] Zhongwei Li, Zhihao Deng, Chang Liu, and Yingsheng Zhang. The composite method of symmetry adapted perturbation theory. 2022.
- [8] Gemma Miralles Adrover. Orbital contributions to the exchange-repulsion energy of atomic and molecular aggregates, bachelor thesis, ebrerhard-karls universität-tübingen. 2018.
- [9] Robert S Mulliken. Structures of complexes formed by halogen molecules with aromatic and with oxygenated solvents. *Journal of the American Chemical Society*, 72(1):600–608, 1950.
- [10] Frank Neese. Software update: The orca program system—version 5.0.3, 2022.
- [11] Trent M Parker, Lori A Burns, Robert M Parrish, Alden G Ryno, and C David Sherrill. Levels of symmetry adapted perturbation theory (sapt). ii. convergence of interaction energy components. *The Journal of chemical physics*, 140(9):094106, 2014.
- [12] Mutasem Omar Sinnokrot and C David Sherrill. Highly accurate coupled cluster potential energy curves for the benzene dimer: sandwich, t-shaped, and parallel-displaced configurations. *The Journal of Physical Chemistry A*, 108(46):10200–10207, 2004.

- [13] Mutasem Omar Sinnokrot and C David Sherrill. Highly accurate coupled cluster potential energy curves for the benzene dimer:sandwich, t-shaped, and parallel-displaced configurations. *The Journal of Physical Chemistry A*, 108(46):10200–10207, 2004.
- [14] Daniel GA Smith, Lori A Burns, Andrew C Simmonett, Robert M Parrish, Matthew C Schieber, Raimondas Galvelis, Peter Kraus, Holger Kruse, Roberto Di Remigio, Asem Alenaizan, et al. Psi4 1.4: Open-source software for high-throughput quantum chemistry. *The Journal of chemical physics*, 152(18), 2020.
- [15] Anthony Stone. *The theory of intermolecular forces*. Oxford University Press, 2013.
- [16] Peifeng Su, Zhen Tang, and Wei Wu. Generalized kohn-sham energy decomposition analysis and its applications. *Wiley Interdisciplinary Reviews: Computational Molecular Science*, 10(5):e1460, 2020.
- [17] Krzysztof Szalewicz, Bogumił Jeziorski, and Stanisław Rybak. Perturbation theory calculations of intermolecular interaction energies. *International Journal of Quantum Chemistry*, 40(S18):23–36, 1991.
- [18] Jonathan E Thirman. *A Second-Order Møller-Plesset Perturbation Theory Energy Decomposition Analysis for Intermolecular Interactions: Design, Implementation, and Application*. University of California, Berkeley, 2017.
- [19] Helen Hoi Yan Tsui. *New models for intermolecular repulsion and their application to Van Der Waals complexes and crystals of organic molecules*. University of London, University College London (United Kingdom), 2001.